Research Paper

Multi-objective optimization of a solar-assisted heat pump for swimming pool heating using genetic algorithm

Allan R. Starke[a],*, José M. Cardemil[b], Sergio Colle[a]

[a] LEPTEN – Laboratory of Energy Conversion Engineering and Energy Technology, Department of Mechanical Engineering, Federal University of Santa Catarina (UFSC), Florianópolis, Brazil
[b] Mechanical Engineering Department, Universidad de Chile, Beauchef 851, Santiago, Chile

HIGHLIGHTS

- Design of four different i-SAHP for pool heating with multi-objective optimization.
- Solar-assisted configurations present significant improvements in performance.
- Same levels of comfort at lower ALCCs than the ASHP configuration.
- Trade-off curves helps define a solution based on the willingness to pay for a specific comfort level.
- Practically all solar-assisted configurations presented positive values of ALCS.

ARTICLE INFO

ABSTRACT

A proper assessment of heating systems for swimming pools should evaluate the compromise between comfort level and the willingness to pay for it. The present work presents a multi-objective optimization of indirect solar assisted heat pump systems for outdoor swimming pool heating. Four different configurations are reported; (air-to-water heat pump and three solar assisted heat pumps, air-to-water, water-to-water and a dual-source); and evaluated in six different locations (three location in Chile: Antofagasta, Santiago, and Concepción; and three locations in Brazil: Brazilia, São Paulo, and Florianópolis). The methodology approach configures two objectives optimization, the minimization of the Annualized Life Cycle Cost (ALCC) and the maximization of the comfort level offered by the swimming pool. The optimization scheme consists of using a combination of tools: the energy-savings potential of i-SAHP are evaluated using the TRNSYS software in combination with GenOpt; and the economic modeling and optimization are performed in the MATLAB environment, using an approximation model and variant of NSGA-II genetic algorithm for building the Pareto frontiers. The optimization results demonstrate that solar-assisted configurations present significant improvements in performance for almost all locations, reaching the same levels of comfort at lower ALCCs when compared with the ASHP configuration.

1. Introduction

The use of heating systems for swimming pools has grown significantly recent years and currently it represents a significant share of energy consumption in domestic applications [1]. However, the proper assessment of these systems is commonly hindered by difficulties for evaluating the comfort level that offer and its compromise with the cost that represent. To aid the decision by the consumer, several authors have developed simulation models for assessing the performance of swimming pool heating systems [2–4]. Recently, Starke et al. [5], presented an extensive review of the methodologies for assessing the performance of swimming pool heating systems, as well as different

applications and modeling solar-assisted heat pump simulations. The authors presented a case study considering three configurations of solar-assisted heat pumps for swimming pool heating in Southern Brazil. The simulations were performed using TRNSYS [6] software and the results were compared against a conventional heat pump. The annual simulations indicated that a solar-assisted heat pump can achieve significantly better performance than a conventional heat pump system. The proposed schemes reduced energy consumption up to 48%, and the systems can achieve a seasonal performance factor (annual coefficient of performance) between 6.7 and 8.2. The proper design of the solar field and heat pump was determined through a detailed economic assessment, combining cost and energy performance of all system

components. This assessment indicated that only the solar assisted-air source heat pump and solar assisted-dual source heat pump were economically feasible.

Although the feasibility of solar-assisted heat pumps for swimming pool heating was already addressed in previous publications, it is mainly focused on a specific case study or on just meeting a specific heat load (temperature set-point). Variations in pool temperature yield changes on the comfort level offered, leading to a change on the energy costs for meeting those requirements. Hence, a higher comfort level requires a different design of the system, which can result in larger capital costs. Based on that, it is interesting that the consumer can assess his/her compromise between the expected comfort level and the willing to pay for it. This scenario results in a clear trade-off between comfort level and cost, which can be addressed by a multi-objective optimization.

In this context, the present study presents the further development of the work reported in [5], which aims to demonstrate the usefulness of multi-objective optimization for analyzing different configurations of indirect solar assisted heat pumps (i-SAHP) for outdoor swimming pool heating, operating in different locations. The objectives to be optimized are the Annualized Life Cycle Cost (ALCC), which should be minimized, and the comfort level offered by the swimming pool, which should be maximized. Since selecting an optimum solution depends on the preferences and criteria of the decision maker, an example of the decision-making process to select a final optimal solution from the Pareto frontier is presented. The final results are obtained using the linear programming technique for multidimensional analysis of preference (LINMAP) decision making approach [7,8].

Multi-objective optimization has been extensively used for the design and optimization of thermal systems [9–14]. Lazzaretto and Toffolo [9] demonstrated the use of an evolutionary algorithm to optimize and design a thermal system using energy, economy, and environment as objective functions. Magnier and Haghighat [10] presented a methodology to optimize the thermal comfort and energy consumption in a residential house. Because optimizing a building is a time-consuming process, the authors used an artificial neural network (ANN) to characterize building behavior, and a multi-objective genetic algorithm to perform the optimization procedure. The results showed a significant reduction in energy consumption and an improvement in thermal comfort, revealing several potential designs and a wide degree of compromise between thermal comfort and energy consumption. Ahmadi et al. [11] performed a multi-objective optimization to design a combined cycle power plant considering exergetic, economic, and environmental factors. They showed that the optimization procedure for a combined cycle power plant requires the utilization of multi-objective optimization to be practical and comprehensive. Asadi et al. [12] described a multi-objective optimization scheme for retrofitting a building. The methodology consisted of optimizing the retrofit cost, energy savings, and thermal comfort of a residential building. The results demonstrated the practicability of providing decision support in an actual setting, allowing simultaneous consideration of all available combinations of retrofit actions. Khorasaninejad and Hajabdollahi [14] performed a design optimization of a solar-assisted heat pump using a multi-objective Particle Swarm Optimization algorithm. The total annual cost and coefficient of performance were considered as objective functions. The heat pump was optimized separately for five working fluids and considered five independent parameters: the solar collector surface area, evaporator pressure, condenser pressure, capacity of the heat storage tank, and the level of superheating/subcooling in the evaporator/condenser. Karathanassis et al. [13] presented a methodology to optimize and design a micro-channel plate-fin heat sink to cool a linear parabolic trough Concentrating Photovoltaic/Thermal (CPVT) system. The authors construct a surrogate function for the thermal resistance and the pressure drop of the heat sink, which are considered as the objective functions for the multi-objective optimization through a genetic algorithm.

Based on the aforementioned advantages that multi-objective optimization offers for analyzing thermal systems and the aiming to facilitate convergence, the proposed methodological approach consists of using a combination of tools for the optimization scheme. The energy-savings potential of four i-SAHPs for outdoor swimming pool heating are evaluated using the TRNSYS [6] energy simulation software in combination with GenOpt [15] to automatically run different scenarios. Economic modeling and optimization procedures are performed in the MATLAB environment [16], which allows for a fast and efficient method of multi-objective optimization when using a sort of approximation of the fitness function (performance calculations) [17].

A swimming pool of 36 m³ and 24 m² of water surface is adopted for the case study, in which the solar field area and heat pump capacity are designed by the optimization process for three locations in Chile (Antofagasta, Santiago, and Concepcion) and three locations in Brazil (Brazilia, São Paulo, and Florianópolis). These locations have different climatic conditions, allowing us to show the usefulness of the methodology proposed.

2. System description

The present study assess the same four heating schemes proposed in [5]: an air source heat pump system (ASHP, Fig. 1a), considered as the reference case; a solar-assisted air source heat pump (SA-ASHP, Fig. 1b), configuring the solar collectors connected in parallel to an air source heat pump; a solar-assisted water source heat pump (SA-WSHP, Fig. 1c) where the collectors are coupled in series to a water-to-water heat pump; and a dual-source heat pump (SA-DSHP, Fig. 1d) which considers two evaporators (one in series to the solar collectors and an
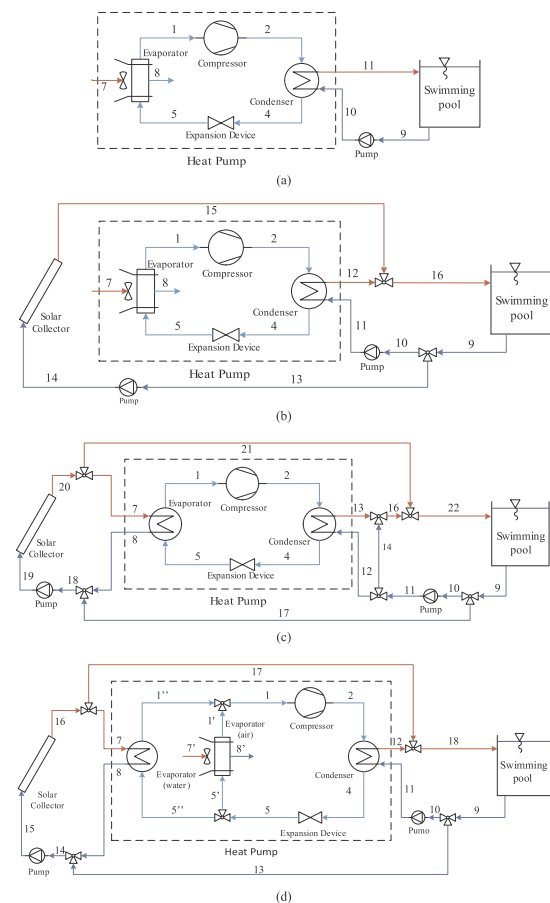

Fig. 1. Schematic diagram of (a) ASHP, (b) SA-ASHP, (c) SA-WSHP, and (d) SA-DSHP systems.

air source evaporator). The details of each configuration, circulation schemes, control strategies and mathematical models of system's components are fully described in [5].

3. Methodology

The methodology employed in the current study consists of using a combination of tools, where TRNSYS and GenOpt are used to design the numerical experiments and build a performance database for each configuration. Then, the MATLAB environment is employed to read these databases, perform a post-processing procedure, build a surrogate model, and perform the optimization routine using a genetic algorithm.

TRNSYS is used to assess the thermal performance of each configuration by means of an annual simulation, considering a transient model using a 6-min time step an hourly meteorological data. In addition, standard TRNSYS relative tolerance of 0.001 for convergence of input and outputs variables and for the numerical integration process were adopted. TRNSYS consists of a transient solver with a modular structure that allows for solve and analyze different configurations of complex energy systems with high flexibility.

Although GenOpt is an optimization program, it is not capable of directly handling a multi-objective optimization. Therefore, GenOpt is used to automate the TRNSYS runs and generate a performance database. Combined with TRNSYS, GenOpt can be easily configured to automatically vary the independent variables, generate the input files, run TRNSYS, and save the results.

Finally, the performance database for each configuration is loaded in MATLAB, where the two objective functions are assessed (Annualized Life Cycle Cost (ALCC) and the comfort level). Then, a surrogate model (e.g., response surface approximation model) is built for each of these objective functions, and a genetic algorithm (GA) is applied to solve the optimization model. This approach is a very efficient method to reduce the intrinsic computational time of GA and complex thermal system simulations [10].

There are several methods to create surrogate models (i.e., polynomial, kriging, neural networks, and support vector machines). However, there is no common opinion as to which method performs better than the others, since the performance of the approximation depends on the nature of the problem addressed and more than one performance measurement can be considered [17]. In the present study, the authors chose a linear interpolation method (without extrapolation) to build the surrogate models, developing a surface in the form $v = F(x, y)$ for each objective function. As mentioned before, the design variables are the solar field area and the heat pump capacity. A linear interpolation was chosen to avoid local minimums in the approximate model, as suggested in [17]. To ensure a good approximation within the interpolation method, 189 numerical cases were evaluated in TRNSYS (a mesh composed by 27 points for the collector area and 7 heat pump capacities), which are equally spaced in the analyzed domain. The solar field size ranges from $1.1\,m^2$ to $144\,m^2$, with a step of 6 modules of $1.1\,m^2$, in this way it is possible to asses small and significantly large solar fields (six times the pool area), larger that a usual available space in dwellings. While, the heat pumps are scaled, with a step of 2.3 kW, from a small equipment (2 kW) to the largest equipment that can be installed without the need of three-phase electric installation.

3.1. Thermal modeling

The mathematical models used to perform the simulations are fully described in [5]. Yet, it's worth mentioning the main TRNSYS components used to build the simulations. The TRNSYS standard library contains types suitable to model most of the components of the systems studied herein (e.g., solar collector, pumps, valves, and controllers). An exception is the swimming pool, for which an additional type was implemented based on the model of an external pool developed by Hahne and Kubler [2]. Regarding the heat pump, the simulation was

conducted using a performance matrix, as most of the types employed for modeling conditioning equipment in TRNSYS. This performance matrix was estimated through a thermodynamic model developed using Engineering Equation Solver [18].

Each component was individually validated: the solar field was simulated using an experimental efficiency curve [19]; the performance matrix of the heat pump was compared against catalog data [20]; and the swimming pool model was validated by Hahne and Kubler [2] and recently by Ruiz and Martínez [3].

3.2. Objective functions

3.2.1. Comfort level

As a metric to measure the comfort level offered by the pool over a year, the probability that the pool's water temperature is at specified range is adopted, such as 26 °C to 30 °C. Then, this measurement can be maximized to ensure that the temperature of the pool presents a high probability of being within the specified temperature range. Therefore, this metric can be used for designing a heating system that guarantees a specific comfort level. The probability of the water pool temperature is calculated using a cumulative distribution function of the year-long simulated water pool temperature. Hence, the comfort level can be expressed as

$$\text{Comfort} = P(26\,°\text{C} \leqslant T_p \leqslant 30\,°\text{C}) = (F_{T_p}(30\,°\text{C}) - F_{T_p}(26\,°\text{C})) \tag{1}$$

where P is the probability, T_p is the pool temperature, and F_{T_p} is the cumulative distribution function of the simulated pool temperature. The comfort level should be maximized; however, to facilitate the optimization process, the objective function is rewritten in a way that it could be minimized, i.e., (1−Comfort), which could be interpreted as the probability discomfort range.

3.2.2. Annualized life cycle cost

The Annualized Life Cycle Cost (ALCC) is an economic measure for an energy system that considers all costs over its lifetime (i.e., initial investment, operations and maintenance, cost of fuel, and cost of capital), which represents an average yearly expenditure cash flow. To estimate this economic figure the P_1 and P_2 method is chosen, as recommended in [21] and expressed as follows:

$$ALCC = \frac{[F_{hp}C_{F,ele}P_1]Q_L + [(1 + C_{inst,A})C_A A_c + (1 + C_{inst,hp})C_{hp} + C_E]P_2}{PWF(N_e, 0, d)} \tag{2}$$

where $C_{F,ele}$ is the electricity tariff, F_{hp} is the energy ratio between the heat pump electricity consumption and the pool thermal load (Q_L). $C_{inst,A}$ and $C_{inst,hp}$ are the installation costs of the solar field and the heat pump as a percentage of the acquisition cost of each equipment, respectively. C_A is the area-dependent cost, A_c is the solar field area, C_{hp} is the heat pump cost, and C_E represents local additional costs. P_1 is the term associated with the life-cycle fuel cost, P_2 is the term associated with the life-cycle cost of the initial investment and its expenditures, and $PWF(N_e, 0, d)$ is the present worth factor for "annualizing" the cash flow. Additionally, the following considerations were adopted for the P_1 and P_2 methods: no income is produced by the operation of the system, no loan or financing schemes are considered, and no net property tax is applied to the installation.

3.3. Optimization framework

As mentioned before, the optimization framework of this study consists of several steps. First, a database of cases is developed using the simulated data from TRNSYS and GenOpt, which consists of performance maps for each configuration and location, generated as a function of the independent variables. Then, a surrogate model is created for each of these cases in MATLAB. Finally, a Pareto frontier is determined using a multi-objective genetic algorithm.

3.3.1. Surrogate model and validation

The first step to create the surrogate model is to generate a performance map through a parametric analysis. An equally spaced mesh is used to create a decision variable space in terms of the solar field area (A_c) and the scale factor of the heat pump (SF_{HP}).

The performance map consists of 189 TRNSYS evaluations, with 27 numeric values for the solar collector area (ranging from $1.1\,\text{m}^2$ to $144\,\text{m}^2$, with a step of 6 modules of $1.1\,\text{m}^2$) and 7 heat-pump scale factors (ranging from 0.2 to 1.4). The heat pumps are scaled from a small equipment (2 kW) to the largest equipment that can be installed without the need of three-phase electric installation. The scale factor is used to assess the effect of the capacity of the heat pump on the system. Therefore, a commercial heat pump is considered as the reference case. The rating parameters of this heat pump were linearly scaled, i.e., the volumetric displacement rate of the compressor and the valve flow coefficient. Using this approach, it is possible to scale equipment in a physically consistent method and range the nominal heat pump capacity from 3 kW to 17 kW.

A performance map was created for each of the four configurations and six locations. These data were used to build a performance database, and the economic assessment and comfort level calculations were later incorporated into the database. Therefore, the user can select the location and configuration, and create a surrogate model for each objective function. Since the performance map was created with a considerably large amount of data – 189 data points for only two independent variables – it is possible to use an interpolation tool rather than the polynomial function usually used in surface methods.

The MATLAB *griddedInterpolant* class [22] is used to create an interpolant surface ($v = F(x, y)$), which is used in the optimization algorithm to calculate the fitness evaluation at any query point (x_q, y_q). The interpolated value at a query point is based on a linear interpolation of the values at neighboring grid points in each respective dimension, and no extrapolation is allowed.

In order to validate the surrogate model, a sample of 15 cases, different from the original and randomly selected from the 2D decision space, is used. The distributions of the validation points are depicted in Fig. 2.

The Mean Absolute Percentage Error (MAPE) for the approximation models was considered acceptable, since it shows 0.5% for ALCC and 1.38% for the comfort level. Furthermore, both models present coefficients of determination R^2 close to 0.998. The differences between the simulated results and the values predicted by the interpolation models are illustrated in Fig. 3, which shows predicted values between ± 3%, characterizing a good agreement between the simulation and approximation model.

3.3.2. Optimization method

Energy, economic, and environmental modeling usually leads to nonlinear optimization problems or to mixed integer nonlinear (MINLP) optimization problems [8]. Objective functions that involve solving a
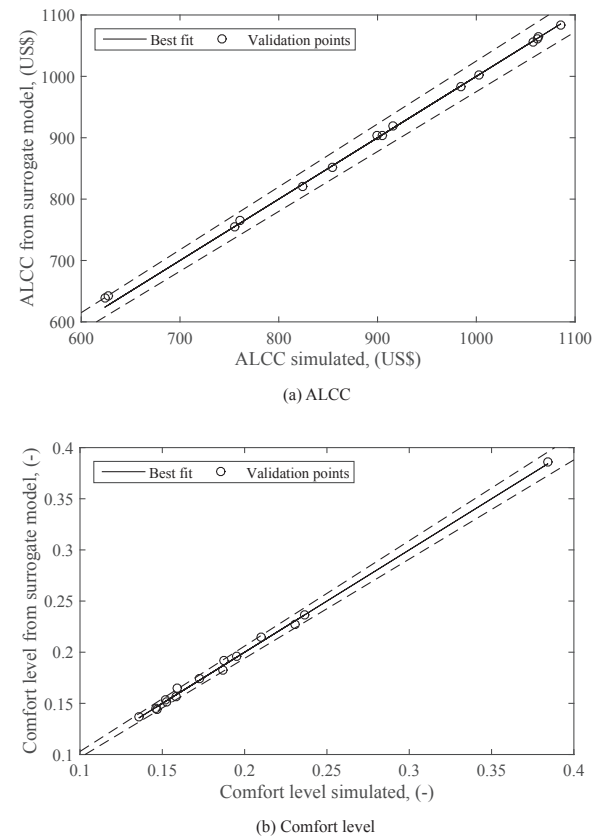

(a) ALCC

(b) Comfort level

Fig. 3. Dispersion diagrams of surrogate models.

system of partial and ordinary differential equations, coupled with algebraic equations, in general are an approximating function since the equation system cannot obtain an exact solution. Because of the precision of the numerical solvers, a perturbation in the independent variables causes a change in the sequence of solver iterations, which causes the objective function to be discontinuous and therefore not continuously differentiable. This is typically the case when the objective function is calculated by a thermal simulation program such as TRNSYS.

Based on this, it is necessary to consider an optimization algorithm that is suited to problems where traditional optimization techniques break down, for example, owing to the irregular structure of the search domain (the absence of gradient information). As also an algorithm that avoid local optima, which ensure the determination of global optimum. For the case of multi-objective optimization, an algorithm that yields Pareto optimal points that do not depend on the function continuity or domain convexity is also necessary. In that context, Multi-Objective Evolutionary Algorithms (MOEA), which include the GA, have been extensively used by researchers [9,23,10,11,24,8,13]. The genetic algorithm applies an iterative stochastic search strategy to find an optimal solution, which imitates in a simplified manner the principles of biological evolution. This is a robust and flexible approach that can be applied to a wide range of learning and optimization problems [25,11,26,27].

In this study, the MATLAB solver *gamultiobj* [16] was adopted. It uses a controlled elitist genetic algorithm (a variant of NSGA-II [28]). Furthermore, a hybrid scheme is used, so *gamultiobj* runs with a small number of generations to get near an optimum front. Then, this solution is used as an initial point for a second optimization procedure, which uses *fgoalattain* (solves the goal attainment problem). Using the hybrid function improves the certainty of finding an optimal Pareto front, but it may lose the diversity of the solution. This can be overcome by running *gamultiobj* again with the final population returned during the
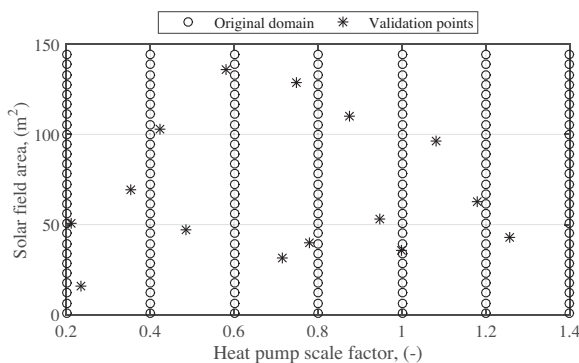

Fig. 2. Random validation points and decision space.

Table 1
Genetic algorithm parameters.

Population size	Pareto fraction	Hybrid function	Tolerance	Max Generation
500	1.0	*fgoalattain*	1×10^{-4}	2000

last run, without any hybridization. The optimization algorithm runs using default parameters, and the exceptions are summarized in Table 1.

The optimization problem was formulated so that both objective functions should be minimized. Therefore, it is expressed as follows:

$$\text{Minimize:} \begin{cases} F_1(\vec{x}) = ALCC(\vec{x}), \\ F_2(\vec{x}) = (1 - \text{Comfort}(\vec{x})), \end{cases}$$

Subject to:

$$x_i^L <= x_i <= x_i^U, \quad i = 1, 2. \tag{3}$$

where F_1 and F_2 are the two objective functions, and $\vec{x}$ is a vector of n independent variables: $\vec{x} = (A_c, SF_{HP})^T$. It is observed that the optimization problem is only subject to variable constraints, which delimits the decision space ($\vec{x}$) by its lower (x_i^L) and upper (x_i^U) values. A first optimization was set up using the methodology described above, and the results are depicted in Fig. 4 for Florianópolis and SA-ASHP. These results show the Pareto front and the feasible performance space, indicating that the optimization algorithm results in an accurate prediction of the Pareto frontier.

4. Simulation parameters

4.1. Weather data

Six different locations in South America were considered: three in Chile (Antofagasta, Santiago, and Concepción), and three in Brazil (Brasilia, São Paulo, and Florianópolis). The main characteristics of these locations are summarized in Table 2.

4.2. Solar field

The collector array consisted of uncovered-polymeric solar collectors (1.1 m²) connected in series and oriented facing the equator with a slope angle equal to the latitude plus 10 degrees. The efficiency parameters are $F_R(\tau\alpha)_n = 0.7327$, $F_R U_L = 19.3 \, \text{W/(m}^2 \, \text{K)}$, and $F_R U_{LT} = 0$ [19]. The mass flow rate under the test conditions is $\dot{m}_{test} = 0.0182 \, \text{kg/(m}^2 \, \text{s)}$.

4.3. Heat pump

A commercial water source heat pump was considered as a reference case and was scaled to assess the effect of the capacity on the
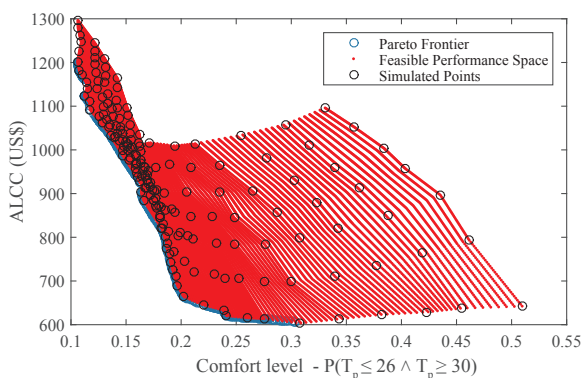
Table 2
Main characteristics of selected locations.

Location	Latitude	Longitude	Altitude, (m.a.s.l.)	Yearly total GHI, (kWh/m²)	Source
Antofagasta	23.43°S	70.43°W	40	1821	Meteonorm
Santiago	33.38°S	70.78°W	521	1383	Meteonorm
Concepcion	36.77°S	73.05°W	12	1526	Meteonorm
Brasilia	15.87°S	47.92°W	1172	2092	SWERA
São Paulo	23.65°S	46.65°W	760	1870	SWERA
Florianópolis	27.53°S	48.52°W	3	1590	SWERA

Table 3
Scaled heat pump capacity and electrical power at rated conditions

		Scale factor (SF)						
		0.2	0.4	0.6	0.8	1.0	1.2	1.4
Water Source	Capacity (kW)	2.3	4.7	7.1	9.5	11.9	14.3	16.6
	Power (kW)	0.3	0.8	1.2	1.6	1.9	2.4	2.8
Air Source	Capacity (kW)	2.4	3.9	5.8	7.8	9.7	11.6	13.6
	Power (kW)	0.3	0.9	1.3	1.7	2.2	2.6	3.1

system. The heat pump has a nominal heating capacity of 12.9 kW. The rating parameters of this heat pump were linearly scaled, whereas the capacities and power consumption as a function of SF are presented in Table 3.

For the SA-ASHP, the water mass flow rate through the collectors was calculated as a function of the total area of the solar field and the test mass flow rate. Meanwhile, for the SA-WSHP, the mass flow rate through the collectors was assumed to be equivalent to the minimal flow rate admissible at the heat pump evaporator (0.6 kg/s).

4.4. Pool

A standard domestic pool of 36 m³ and 24 m² of water surface is considered. Regarding the pool cover, a floating low-density polyethylene blanket is considered, whose top surface is highly smooth and whose lower surface has air pockets to improve buoyancy. This cover has 3.26 mm of thickness and thermal conductivity of 0.02856 W/(m K). An absorptivity and emissivity of 0.9 was assumed.
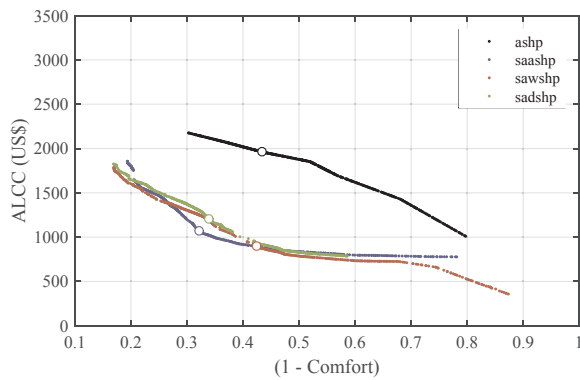
4.5. Economic

The equipment costs and economic considerations for the analysis are summarized in Table 4.

It is worth mentioning that the air source and the water source heat pumps have the same initial cost, which can be expressed in US$ as function of the scale factor:
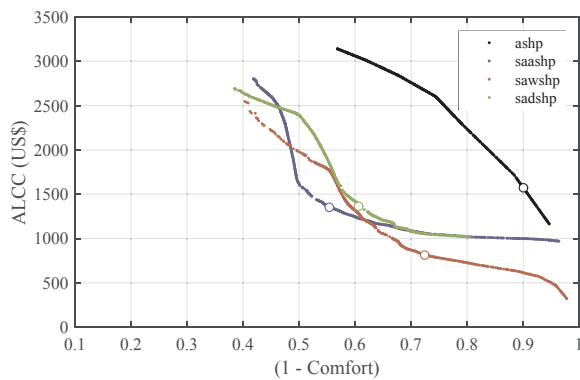
$$C_{hp} = 897.4 SF + 1038.5 \tag{4}$$
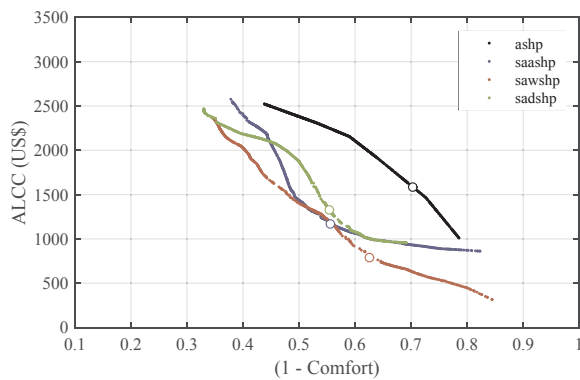
Table 4
Economic considerations adopted.

Parameter	Value
Period of economic analysis, N_e	20 years
Insurance and maintenance costs, M_s	2%
Discount rate, d	7.25%
Inflation rate of fuels, I_F	4%
Resale value, R_v	10%
Electricity tariff, $C_{F,ele}$	0.16 US$/kWh
Area-dependent cost, C_A	52 US$ m²
Pool cover cost, C_E	320 US$
Solar field installation cost, $C_{inst,A}$	10%
Heat pump installation cost, $C_{inst,hp}$	30%

Fig. 4. Feasible performance space and the Pareto front obtained from GA.

(a) Antofagasta

(a) Brasília

(b) Santiago

(b) Florianópolis

(c) Concepcion

(c) São Paulo

Fig. 5. Pareto optimal frontiers for Chilean locations. Optimal design selected by LINMAP decision maker is highlighted.
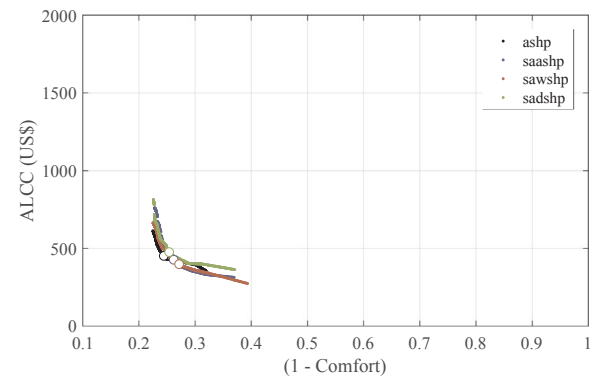
Fig. 6. Pareto optimal frontiers for Brazilian locations. Optimal design selected by LINMAP decision maker is highlighted.

For the dual-source heat pump, the cost was specified at 20% higher than that considered for the air and water source heat pumps.
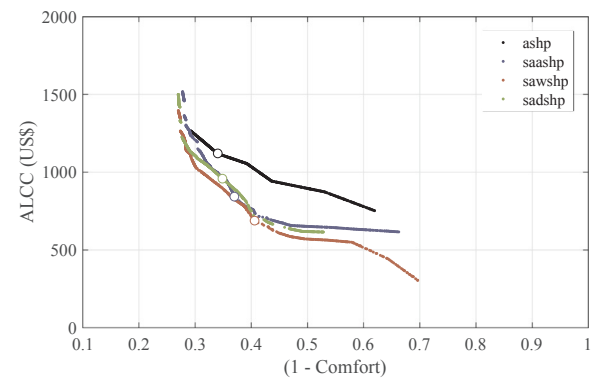
5. Results

Pareto optimal frontiers for each configuration and location are illustrated in Figs. 5 and 6, clearly revealing the conflict between the two objective functions analyzed. For all studied cases, the Pareto fronts are composed of 500 optimal points and present a homogeneous spread between the extreme solutions.

For Chilean locations, the optimal solutions range from an ALCC of 500 US$ to 3000 US$. On the other hand, the discomfort (1−Comfort) ranges between 0.2 and 0.9 for Antofagasta, from 0.45 to 1 for Santiago, and between 0.35 and 0.8 for Concepción, since these last two locations present lower yearly average ambient temperatures.
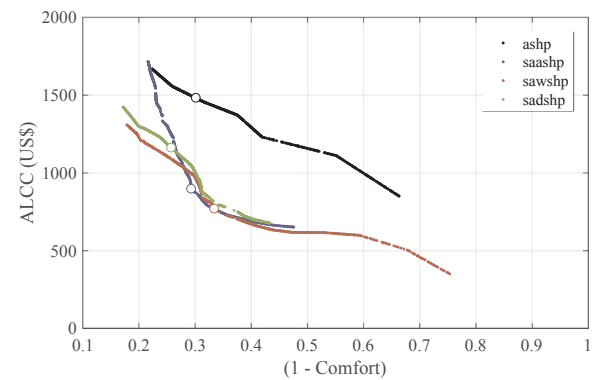
For Brazilian locations, the optimal solutions range from an ALCC of 500 US$ to 1500 US$ and discomfort of 0.2–0.7 for Florianópolis and São Paulo. Brasilia has a significantly higher yearly average ambient temperature; therefore, it presents a significantly different range of optimal solutions ranging from an ALCC of 250 US$ to 750 US$ and discomfort between 0.2 and 0.4. Based on these ranges for the optimal solutions and the high trade-offs between the objective functions, the usefulness of multi-objective techniques to properly design these systems seems clear. Furthermore, this allows consumers to decide on a final solution based on their willingness to pay for a specific level of comfort.

It is observed that the solar-assisted configurations present significant improvements in performance for almost all locations, reaching similar levels of comfort at lower ALCCs when compared against the ASHP configuration. The exception is Brasilia, in which all configurations present almost identical Pareto fronts as a consequence of the higher yearly average ambient temperatures. In addition, the fronts are

located at the lower left corner of the chart, indicating that a heating system is practically unnecessary for a pool located in that city.

The fronts for Antofagasta (Fig. 5a) show optimal fronts crossing each other, which indicates that the best configuration depends on the desired comfort level. For instance, considering discomfort ($1-comfort$), at a value lower than 0.47 the SA-WSHP performs a lower ALCC, and for a discomfort between 0.47 and 0.6 the SA-ASHP performs better. Finally, for discomfort higher than 0.6, the SA-WSHP again performs better. Similar behavior is observed for all locations where the crossing points vary for each location.

From an observation of the figures, it is possible to corroborate that the weather conditions have a major effect on the Pareto optimal frontiers. Therefore, the configurations should be properly designed in terms of comfort and installation costs for each location.

5.1. Final optimal solutions through decision-making

To fully demonstrate the usefulness of the optimization process, a decision-making method is used to select a final optimal solution from the Pareto frontiers. Finally, the optimal solutions, including the reference configuration (ASHP), are compared with each other.

A method for final decision-making is required since the dimensions of the two objective functions are different. The dimensions and scales of the objective functions should be unified. In this study, the Linear Programming Technique for Multidimensional Analysis of Preference (LINMAP) developed by Srinivasan and Shocker [7] was adopted. In this approach, each objective function is subjected to a Euclidian non-dimensionalization [8], which is defined as follows:

$$F_{ij}^n = \frac{F_{ij}}{\sqrt[2]{\sum_{j=1}^{m}(F_{ij})^2}}$$

(5)

where F_{ij}^n is the "i" nondimensionalized objective, and F_{ij} denotes the "j" points of the "i" objective on the Pareto frontier.

After nondimensionalization of the objective functions, the LINMAP method is applied. This consists of calculating the spatial distance between each point on the Pareto frontier and an ideal point, as follows:

$$d_j = \sqrt[2]{\sum_{i=1}^{n}(F_{ij}-F_i^{Ideal})^2}$$

(6)

where d_j denotes the distance between the "j" point and the ideal point, while "i" stands for each objective and n denotes the number of objectives. F_i^{Ideal} is the ideal value of the ith objective, obtained from a single-objective optimization. Finally, through the LINMAP method, the final optimal solution is selected as the solution presenting the minimum distance from the ideal point. Therefore,

$$j_{final} \equiv j \in \min(d_j)$$

(7)

For each location and configuration, the two objectives were independently optimized and then used as ideal point to calculate the distances. Fig. 7 illustrates the LINMAP method, as well the ideal point and the final desired optimal solution.

The final optimal solution for each configuration and location are depicted in Figs. 5 and 6, highlighted by a circular marker. Table 5 shows the final optimal solution, listing the values of the two objective functions and the two design variables. Furthermore, the Annualized Life Cycle Savings (ALCS) is also presented, which is calculated as the difference between the ALCCs as follows:

$$ALCS = ALCC_k - ALCC_{ASHP}$$

(8)

where $ALCC_k$ is the annualized life cycle cost of the kth configuration, and $ALCC_{ASHP}$ is the annualized life cycle cost of the ASHP configuration, considered as a reference case. It is worth mentioning that only the final optimal solutions were considered when calculating the ALCS values.

As shown in Table 5, most solar-assisted configurations present positive values of ALCS, indicating savings during the life cycle. The
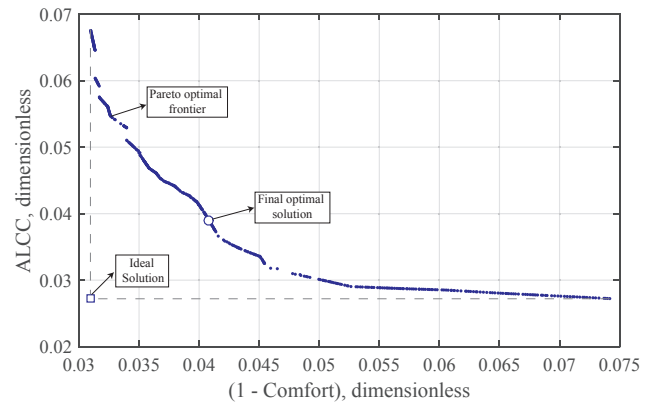

Fig. 7. Pareto optimal frontier of SA-ASHP configuration, for Florianópolis.

Table 5
Final optimal solutions specified by LINMAP decision maker.

		Heat pump scale factor	solar field area	ALCC	(1-Comfort)	ALCS
Brasilia	ASHP	0.60	0.00	430.90	0.25	0.00
	SA-ASHP	0.20	17.97	386.96	0.27	43.94
	SA-WSHP	0.20	17.36	385.17	0.28	45.73
	SA-DSHP	0.20	22.00	449.17	0.26	−18.27
Florianópolis	ASHP	0.94	0.00	1096.71	0.36	0.00
	SA-ASHP	0.21	57.45	795.52	0.38	301.19
	SA-WSHP	0.27	43.36	701.34	0.41	395.36
	SA-DSHP	0.54	44.12	904.53	0.37	192.18
São Paulo	ASHP	1.00	0.00	1455.23	0.31	0.00
	SA-ASHP	0.26	73.93	924.42	0.29	528.47
	SA-WSHP	0.20	53.64	750.36	0.34	702.54
	SA-DSHP	0.22	66.21	882.92	0.31	569.98
Antofagasta	ASHP	1.01	0.00	1964.23	0.43	0.00
	SA-ASHP	0.28	109.77	1218.09	0.30	746.14
	SA-WSHP	0.24	92.17	1076.29	0.37	887.94
	SA-DSHP	0.36	101.24	1257.72	0.33	706.51
Concepcion	ASHP	0.35	0.00	1578.42	0.90	0.00
	SA-ASHP	0.20	102.47	1360.75	0.55	217.67
	SA-WSHP	0.21	56.73	898.17	0.69	680.25
	SA-DSHP	0.21	122.79	1484.42	0.59	94.00
Santiato	ASHP	0.45	0.00	1571.54	0.71	0.00
	SA-ASHP	0.20	104.50	1367.90	0.51	203.64
	SA-WSHP	0.25	43.54	794.48	0.63	777.05
	SA-DSHP	0.20	104.26	1349.84	0.55	221.70

exception is the SA-DSHP for Brasilia, which has a negative value. In addition, all ALCS values for this location are considerably lower than the values observed for the other locations. Furthermore, the LINMAP approach designed final solutions that show the minimal values of the heat pump scale factors (0.2), indicating that the heat pump makes a minor contribution in Brasilia. This conclusion proves that the pool cover and a solar system are enough to keep a swimming pool warm in a location with high to moderate ambient temperatures, such as Brasilia. Regarding the other locations analyzed, the SA-WSHP configurations present the largest savings, with ALCS varying from 395 to 887 US $.

It is also observed that the decision-making process led to solar-assisted configurations combined with a small heat pump, with a scale factor ranging from 0.2 to 0.54. However, if higher values of comfort level are selected, larger heat pumps and solar field collector areas are required. It should be mentioned that one decision-making method has
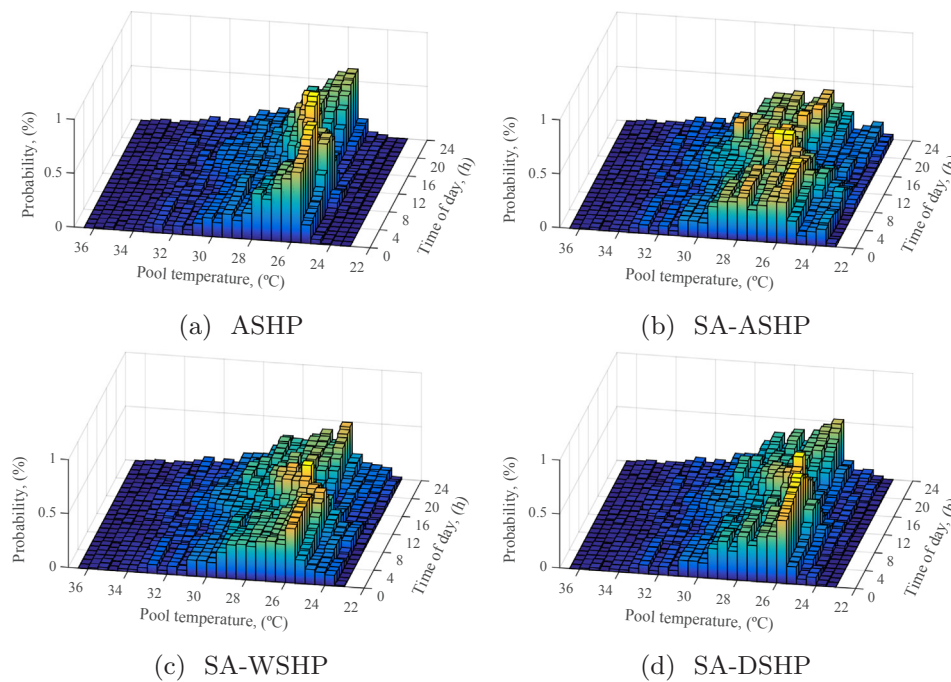
Fig. 8. Probability histogram of pool temperature and time of day of final optimal solution for four configurations, for Florianópolis.

no superiority over the other methods. Indeed, these methods are used to aid decision makers in selecting a final solution. This final decision is based on their professional experience, which should consider the results of the decision-making methods and the willingness of the consumer to pay for a specific comfort level.

Finally, to further assess the final optimal solution, a bivariate probability histogram of pool temperature as a function of the hours of the day is shown in Fig. 8 for Florianópolis. The probability histogram uses a normalization where the height of each bar is the relative number of observations (number of observations in bin per total number of observations). In addition, the sum of all bar heights is equal to a unit. As observed, during the day there is a high probability that the pool temperature is within the comfort range 26–30 °C, including during the night. On the other hand, the histogram also depicts a peak of high probability for temperatures out of the comfortable range, which are concentrated in the early morning and the end of the day. However, this peak is located between 25 °C and 26 °C, which are considerably close to the comfort range and occur during periods of low usage. For temperatures lower than 24 °C, the probability is almost null for ASHP and SA-DSHP configurations, and near 0.1% for early morning and late night for the SA-ASHP and SA-WSHP configurations.

6. Conclusions

This study demonstrates the usefulness of multi-objective optimization for the design process of four different configurations of an i-SAHP for outdoor swimming pool heating, where the solar field area and heat pump capacity were defined during the optimization process. The case study used a swimming pool of 36 m³ and 24 m² of water surface, considering three locations in Chile (Antofagasta, Santiago, and Concepción) and three locations in Brazil (Brazilia, São Paulo, and Florianópolis). The adopted approach is a very efficient method to reduce the intrinsic computational time of the GA and complex thermal system simulations. The objective functions to be optimized are the minimization of the Annualized Life Cycle Cost (ALCC) and the maximization of the comfort level offered by the swimming pool. Therefore, based on these results, a consumer can assess a compromise between a specific comfort level and his or her willingness to pay for it.

Regarding the optimization results, the solar-assisted configurations present significant improvements in performance for almost all locations, reaching the same levels of comfort at lower ALCCs when compared with the ASHP configuration. For Chilean locations, the optimal solutions range from an ALCC of 500 US$ to 3000 US$, and a discomfort level of (1−Comfort) ranging between 0.2 and 0.9 for Antofagasta, from 0.45 to 1 for Santiago, and between 0.35 and 0.8 for Concepción. For Brazilian locations, the optimal solutions range from an ALCC of 500 US$ to 1500 US$ with a discomfort level of about 0.2 and 0.7 for Florianópolis and São Paulo, respectively. Based on the ranges of the optimal solutions and high trade-offs between the objectives, the usefulness of multi-objective techniques to properly design these systems seems clear. Furthermore, it allows the consumer to decide on a final solution based on his or her willingness to pay for a specific level of comfort.

Finally, the Linear Programming Technique for Multidimensional Analysis of Preference is adopted for the final decision-making. Based on this, the values of the two objectives and the two design variables were presented for the final optimal solutions. Practically all solar-assisted configurations presented positive values of ALCS, indicating savings during the life cycle. The final solutions show that the SA-WSHP configurations present the largest savings, with ALCS varying from 395 to 887 US$.

References

[1] W. Kampel, B. Aas, A. Bruland, Characteristics of energy-efficient swimming facilities – a case study, Energy 75 (2014) 508–512, http://dx.doi.org/10.1016/j.energy.2014.08.007.

[2] E. Hahne, R. Kubler, Monitoring and simulation of the thermal performance of solar heated outdoor swimming pools, Sol. Energy 53 (1) (1994) 9–19, http://dx.doi.org/10.1016/S0038-092X(94)90598-3.

[3] E. Ruiz, P.J. Martínez, Analysis of an open-air swimming pool solar heating system

by using an experimentally validated TRNSYS model, Sol. Energy 84 (1) (2010) 116–123, http://dx.doi.org/10.1016/j.solener.2009.10.015.

[4] L.A. Tagliafico, F. Scarpa, G. Tagliafico, F. Valsuani, An approach to energy saving assessment of solar assisted heat pumps for swimming pool water heating, Energy Build. 55 (2012) 833–840, http://dx.doi.org/10.1016/j.enbuild.2012.10.009.

[5] A.R. Starke, J.M. Cardemil, R. Escobar, S. Colle, Thermal analysis of solar-assisted heat pumps for swimming pool heating, J. Braz. Soc. Mech. Sci. Eng. 39 (6) (2016) 2289–2306, http://dx.doi.org/10.1007/s40430-016-0671-y.

[6] S.A. Klein, TRNSYS: A Transient Systems Simulation Program, v. 17; 2013.

[7] V. Srinivasan, A. Shocker, Linear programming techniques for multidimensional analysis of preferences, Psychometrika 38 (3) (1973) 337–369, http://dx.doi.org/10.1007/BF02291658.

[8] H. Sayyaadi, R. Mehrabipour, Efficiency enhancement of a gas turbine cycle using an optimized tubular recuperative heat exchanger, Energy 38 (1) (2012) 362–375, http://dx.doi.org/10.1016/j.energy.2011.11.048.

[9] A. Lazzaretto, A. Toffolo, Energy, economy and environment as objectives in multi-criterion optimization of thermal systems design, Energy 29 (8) (2004) 1139–1157, http://dx.doi.org/10.1016/j.energy.2004.02.022.

[10] L. Magnier, F. Haghighat, Multiobjective optimization of building design using TRNSYS simulations, genetic algorithm, and Artificial Neural Network, Build. Environ. 45 (3) (2010) 739–746, http://dx.doi.org/10.1016/j.buildenv.2009.08.016.

[11] P. Ahmadi, I. Dincer, M.A. Rosen, Exergy, exergoeconomic and environmental analyses and evolutionary algorithm based multi-objective optimization of combined cycle power plants, Energy 36 (10) (2011) 5886–5898, http://dx.doi.org/10.1016/j.energy.2011.08.034.

[12] E. Asadi, M.G. da Silva, C.H. Antunes, L. Dias, A multi-objective optimization model for building retrofit strategies using TRNSYS simulations, GenOpt and MATLAB, Build. Environ. 56 (2012) 370–378, http://dx.doi.org/10.1016/j.buildenv.2012.04.005.

[13] I.K. Karathanassis, E. Papanicolaou, V. Belessiotis, G.C. Bergeles, Multi-objective design optimization of a micro heat sink for Concentrating Photovoltaic/Thermal (CPVT) systems using a genetic algorithm, Appl. Therm. Eng. 59 (1) (2013) 733–744, http://dx.doi.org/10.1016/j.applthermaleng.2012.06.034.

[14] E. Khorasaninejad, H. Hajabdollahi, Thermo-economic and environmental optimization of solar assisted heat pump by using multi-objective particle swam algorithm, Energy 72 (2014) 680–690, http://dx.doi.org/10.1016/j.energy.2014.05.095.

[15] M. Wetter, GenOpt - Generic Optimization Program - User Manual V 2.1.0. Tech. Rep. c; 2008.

[16] The MathWorks Inc. MATLAB R2016b - 64bits, 2015. <http://www.mathworks.com>.

[17] Y. Jin, A Comprehensive survey of fitness approximation in evolutionary computation, Soft Comput. 9 (1) (2005) 3–12, http://dx.doi.org/10.1007/s00500-003-0328-5.

[18] S.A. Klein, EES: Egineering Equation Solver v.10.225. 2017.

[19] S.L. Abreu, J.E. Bastos, Coletores solares planos para líquidos - determinação do rendimento térmico - alo solar 1002. Relatório Técnico - RTTC - 01/01, Tech. Rep.; LABSOLAR/LEPTEN/UFSC; Florianópolis-Brazil; 2001.

[20] Carrier Corporation, AQUAZONE 50PSW036-360: Water-to-Water Source Heat Pump with PURON Refrigerant (R-410A). Tech. Rep.; New York, 2009.

[21] J.A. Duffie, W.A. Beckman, Solar Engineering of Thermal Processes, 3rd ed., John Wiley and Sons, New Jersey, 2006.

[22] The MathWorks Inc, MATLAB griddedInterpolant object, 2017. URL: <https://www.mathworks.com/help/matlab/ref/griddedinterpolant.html>.

[23] J. McCall, Genetic algorithms for modelling and optimisation, J. Comput. Appl. Math. 184 (1) (2005) 205–222, http://dx.doi.org/10.1016/j.cam.2004.07.034.

[24] P. Ahmadi, I. Dincer, Thermodynamic and exergoenvironmental analyses, and multi-objective optimization of a gas turbine power plant, Appl. Therm. Eng. 31 (14-15) (2011) 2529–2540, http://dx.doi.org/10.1016/j.applthermaleng.2011.04.018.

[25] J.S. Arora, Introduction to optimum design, 3rd ed., Academic Press, Amsterdam, 2011 ISBN 9780123813756.

[26] H. Najafi, B. Najafi, P. Hoseinpoori, Energy and cost optimization of a plate and fin heat exchanger using genetic algorithm, Appl. Therm. Eng. 31 (10) (2011) 1839–1847, http://dx.doi.org/10.1016/j.applthermaleng.2011.02.031.

[27] S. Sanaye, H. Hajabdollahi, Multi-objective optimization of shell and tube heat exchangers, Appl. Therm. Eng. 30 (14-15) (2010) 1937–1945, http://dx.doi.org/10.1016/j.applthermaleng.2010.04.018.

[28] K. Deb, S. Agrawal, A. Pratap, T. Meyarivan, A fast elitist non-dominated sorting genetic algorithm for multi-objective optimization: NSGA-II, Parallel Problem Solving from Nature PPSN VI: 6th International Conference Paris, France, Paris, Springer, Berlin, Heidelberg, 2000, pp. 849–858, , http://dx.doi.org/10.1007/3-540-45356-3_83 ISBN 978-3-540-45356-7.